The EMBO Journal (2008) 27, 886–897 | © 2008 European Molecular Biology Organization | All Rights Reserved 0261-4189/08
www.embojournal.org

THE EMBO JOURNAL

Perturbed desmosomal cadherin expression in grainy head-like 1-null mice

Tomasz Wilanowski[1], Jacinta Caddy[1], Stephen B Ting[1], Nikki R Hislop[1], Loretta Cerruti[1], Alana Auden[1], Lin-Lin Zhao[1], Stephen Asquith[2], Sarah Ellis[2], Rodney Sinclair[3], John M Cunningham[4] and Stephen M Jane[1,5,*]

[1]Rotary Bone Marrow Research Laboratories, Melbourne Health Research Directorate, Royal Melbourne Hospital, Parkville, Victoria, Australia, [2]Trescowthick Research Laboratories, Peter MacCallum Cancer Centre, East Melbourne, Victoria, Australia, [3]Department of Dermatology, St Vincent's Hospital, Fitzroy, Victoria, Australia, [4]Department of Pediatrics and Institute of Molecular Pediatric Sciences, University of Chicago, Chicago, IL, USA and [5]Department of Medicine, University of Melbourne, Parkville, Victoria, Australia

In *Drosophila*, the grainy head (*grh*) gene plays a range of key developmental roles through the regulation of members of the cadherin gene family. We now report that mice lacking the *grh* homologue grainy head-like 1 (*Grhl1*) exhibit hair and skin phenotypes consistent with a reduction in expression of the genes encoding the desmosomal cadherin, desmoglein 1 (*Dsg1*). *Grhl1*-null mice show an initial delay in coat growth, and older mice exhibit hair loss as a result of poor anchoring of the hair shaft in the follicle. The mice also develop palmoplantar keratoderma, analogous to humans with *DSG1* mutations. Sequence analysis, DNA binding, and chromatin immunoprecipitation experiments demonstrate that the human and mouse *Dsg1* promoters are direct targets of GRHL1. Ultrastructural analysis reveals reduced numbers of abnormal desmosomes in the interfollicular epidermis. These findings establish GRHL1 as an important regulator of the *Dsg1* genes in the context of hair anchorage and epidermal differentiation, and suggest that cadherin family genes are key targets of the grainy head-like genes across 700 million years of evolution.

The EMBO Journal (2008) **27,** 886–897. doi:10.1038/emboj.2008.24; Published online 21 February 2008
Subject Categories: development
Keywords: cadherins; desmoglein; epidermis; grainy head; hair

Introduction

Although the *grh* gene in *Drosophila* has been linked to a range of developmental events, its predominant expression in the developing cuticle underpins the best-characterized of its mutant phenotypes, which manifest as defects in cuticle integrity and wound repair (Bray and Kafatos, 1991; Mace *et al*, 2005). In the developing wing, *grh* mutants exhibit multiple hairs of abnormal polarity, analogous to the defects observed in mutants of the frizzled-dependent PCP pathway (Lee and Adler, 2004). It has been postulated that a cadherin family member, starry night (*stan*) (also known as flamingo (*fmi*)), is a direct target of GRH. *Grh* mutant clones in the wing also exhibited a delay in hair morphogenesis, which was not mimicked in the *stan/fmi* mutants (Lee and Adler, 2004). Another member of the cadherin gene family directly regulated by *grh* is *E-cadherin/shotgun* (Almeida and Bray, 2005). This regulation is critical in post-embryonic neuroblasts, where *grh* expression is essential for these cells to adopt the stem cell programme appropriate for their position within the central nervous system (Almeida and Bray, 2005).

Our interest has focused on the roles of the three mammalian homologues of *grh*, *Grhl1–3* in the developing epidermis (Wilanowski *et al*, 2002; Ting *et al*, 2003b). All three genes are highly expressed in the developing mouse skin, with differing times of initial and maximal expression (Auden *et al*, 2006). We have previously shown that *Grhl3* is essential for closure of the neural tube (Ting *et al*, 2003a), and for establishing and maintaining the epidermal barrier in mice (Jane *et al*, 2005; Ting *et al*, 2005). This latter function is mediated, in part, through the regulation of a protein/lipid cross-linking enzyme, analogous to the role of *grh* in regulating the *Dopa decarboxylase* gene in the fly cuticle. This finding emphasizes the degree of functional conservation between members of this gene family. We now report a further insight into these functional homologies in our generation and study of mice deficient for *Grhl1*. These animals display a delay in the initial appearance of their coat, coupled with defective hair anchoring to the follicle. They also exhibit palmoplantar keratoderma (PPK) with marked thickening of the epidermal layer of the paws. These phenotypes are unified by the demonstration of diminished expression of the desmosomal cadherin genes coding for desmoglein 1 (*Dsg1*), which we show are direct targets of GRHL1.

Results

Grhl1-null mice exhibit an abnormal hair coat

Mice carrying a targeted *Grhl1* allele were generated as described in the Supplementary data. Genotyping of offspring from *Grhl1*$^{+/-}$ intercrosses at weaning showed that *Grhl1*$^{-/-}$ mice were represented in normal Mendelian proportions. Of 218 pups tested, 53 were +/+ (24%), 120 were +/− (55%), and 45 were −/− (21%). Although the same in size at birth, at weaning, the *Grhl1*$^{-/-}$ pups were smaller than their littermates, and 2 months later these mice displayed no significant difference in size or weight (Supplementary Figure 2). Over 30% of the *Grhl1*$^{-/-}$ pups were devoid of hair at weaning, and the remainder show a marked paucity of

*Corresponding author. Rotary Bone Marrow Research Laboratories, Melbourne Health Research Directorate, Royal Melbourne Hospital, Grattan Street, Parkville, Victoria 3050, Australia.
Tel.: +61 3 93428641; Fax: +61 3 93428634;
E-mail: jane@wehi.edu.au

Received: 22 July 2007; accepted: 31 January 2008; published online: 21 February 2008

 ©2008 European Molecular Biology Organization

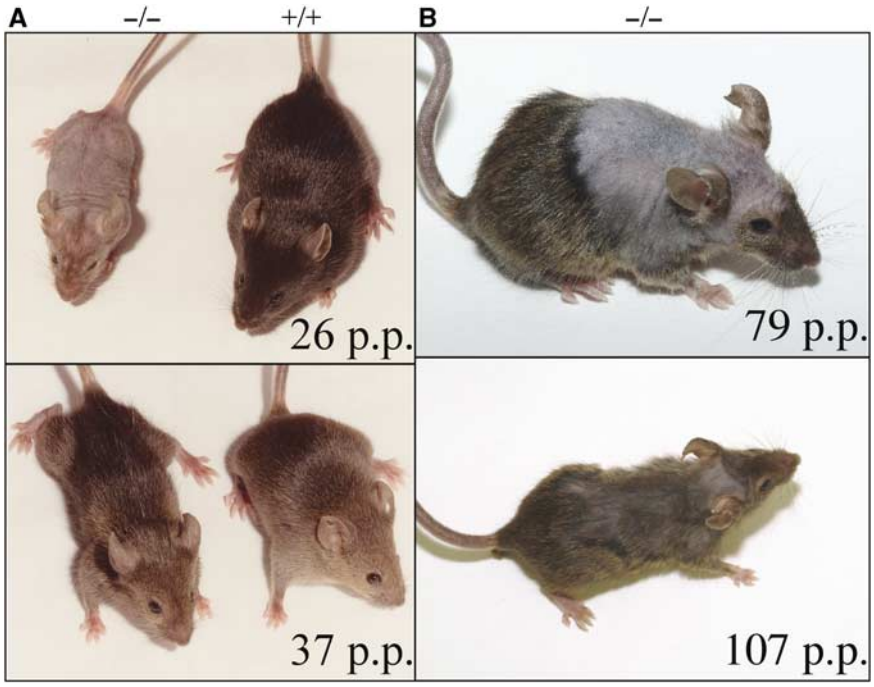

Figure 1 Phenotype of *Grhl1*-deficient mice. (**A**) A representative *Grhl1* mutant (–/–) and wild-type (+/+) littermate photographed at weaning (upper panel). Mice from a separate litter at 37 days (lower panel). (**B**) An example of overgrooming and recovery in a *Grhl1* mutant female. This mouse was housed with other mice when the first photograph was taken. The mouse was photographed again, 3 weeks after being housed in isolation.

hair growth (Figure 1A, upper panel). Growth of whiskers, nails, and teeth were normal in these animals. Later in life, recovery in hair growth was observed; however, all *Grhl1*-null animals exhibited a sparser coat throughout life compared with their wild type littermates. An example of most pronounced hair regrowth is shown in Figure 1A (lower panel). In addition, we noted that many $Grhl1^{-/-}$ mice displayed severe regional hair loss that appeared unrelated to the hair cycle (Figure 1B, upper panel). This aspect of the phenotype was related to grooming by cage-mates, and mice housed in isolation showed sparse hair coats without regional hypotrichosis (Figure 1B, lower panel). This suggested that hair anchoring may be defective in the $Grhl1^{-/-}$ animals. Examination of hair types revealed no differences in frequency or appearance between the wild-type and mutant animals (data not shown). In all other aspects, the $Grhl1^{-/-}$ mice were healthy, with normal fertility and longevity. The formation of the skin barrier and wound healing were unaffected in the $Grhl1^{-/-}$ animals (Supplementary Figure 3; data not shown).

Grhl1 is expressed in the developing epidermis and hair follicles

During embryogenesis, *Grhl1* expression was first detectable by *in situ* hybridization at very low levels in the surface ectoderm at embryonic day 10.5 (E10.5) (Auden *et al*, 2006). By E15.5, *Grhl1* was readily detectable in the skin and in the developing hair germs (Figure 2A). At later time points during development and in the adult, expression of *Grhl1* in the skin was confined to the suprabasal layers of the epidermis and to the hair follicles (Figure 2B). In the whiskers at E17.5, *Grhl1* expression was observed throughout the length of the follicle in the inner root sheath (IRS), but with sparing of the dermal papilla (Figure 2C). These expression patterns were confirmed in mice carrying a *lacZ* reporter gene fused in frame to the first codon of exon 1 of the *Grhl1* gene (Supplementary Figure 1). In E14.5 embryos, β-galactosidase activity was observed in the skin and hair placodes (Figure 2E). In the adult, expression was identified in the suprabasal layers of the epidermis (Figure 2D), IRS of the hair follicle, but not in the dermal papilla (Figure 2F–G). Significant expression of *Grhl1* was also noted during development in other tissues lined by squamous epithelium, including the oral cavity and anal canal. Expression was also observed in several other organs, including lung, kidney, and stomach (Auden *et al*, 2006).

Grhl1-null mice show defective hair anchoring

To determine the underlying pathology in the $Grhl1^{-/-}$ animals, we examined dorsal skin histology in mice at 0, 7, 14, and 21 days (Supplementary Figure 4; data not shown). No abnormalities in the dermal or epidermal architecture were observed at these time points. In particular, the structure and density of hair follicles was identical in both $Grhl1^{-/-}$ and wild-type littermates. Scanning electron microscopy of *Grhl1* mutant hair shafts did not detect any structural differences compared with wild-type hairs (Supplementary Figure 5). Skin sections from areas without obvious hair loss in older mice (3–7 months) were unremarkable, with the exception of sections taken from the palmar or plantar surfaces of the fore and hind paw, respectively (see below). Sections from the hypotrichotic regions of adult mice revealed areas containing empty cysts (Figure 3A). These were reminiscent of the empty dilated telogen hair follicles described in mice carrying a targeted deletion of the desmosomal gene, *Dsg3* (Koch *et al*, 1998).

©2008 European Molecular Biology Organization

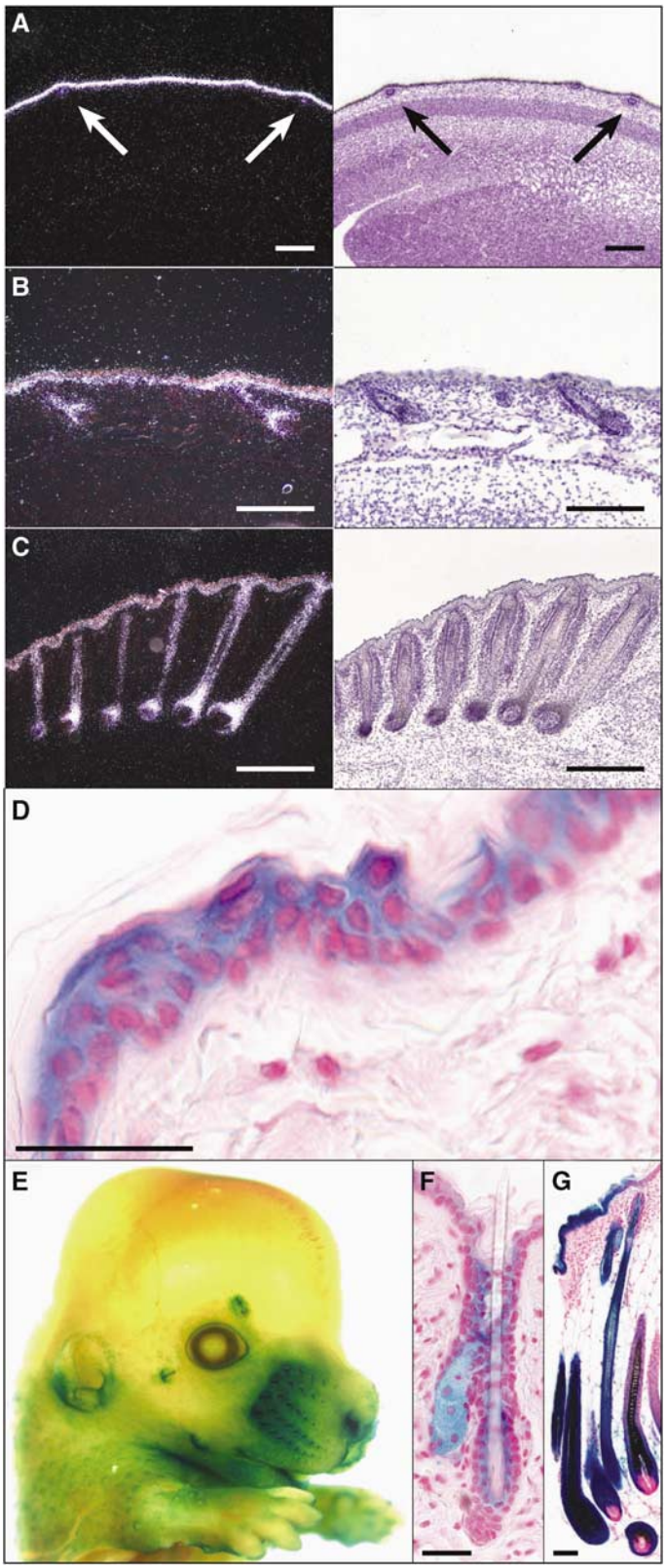

Figure 2 Expression of *Grhl1* in embryonic and adult skin and hair follicles. (**A–C**) Embryonic skin sections probed with *Grhl1*-specific antisense riboprobe. Left: dark field photograph; right: light field photograph. (A) At E15.5, the *Grhl1* transcript is found in the epidermis and in hair germs. Arrows point to the locations of hair germs. (B) At E17.5, the expression extends to the newly formed hair pegs. (C) *Grhl1* expression in whisker pads at E17.5. *Grhl1* is present in the hair follicles except for the dermal papilla. (**D–G**) Staining for β-galactosidase activity in skin from the *Grhl1*$^{-/-}$ mice. (D) Adult epidermis expresses the reporter gene primarily in the suprabasal layers. (E) E14.5 embryo head and upper body detail. At this stage, the β-galactosidase activity is detected throughout the skin and is particularly intense in the hair, ears, and in the lining of the nostrils. (F, G) Adult hair follicles: telogen (F) and anagen (G). In the adult hair follicle, the reporter gene activity is most pronounced in the IRS of the hair follicle, but is absent from the dermal papilla. The scale bars are equivalent to 500 μm in (A–C) and 100 μm in (E–G).

 ©2008 European Molecular Biology Organization

We repeated the histological examination on skin from adult *Grhl1*$^{-/-}$ mice fixed in 70% ethanol. Processing in this way has been shown to display clefts between the IRS and outer root sheath (ORS) in Dsg-deficient mice that were not apparent following formalin fixing (Hanakawa *et al*, 2004).

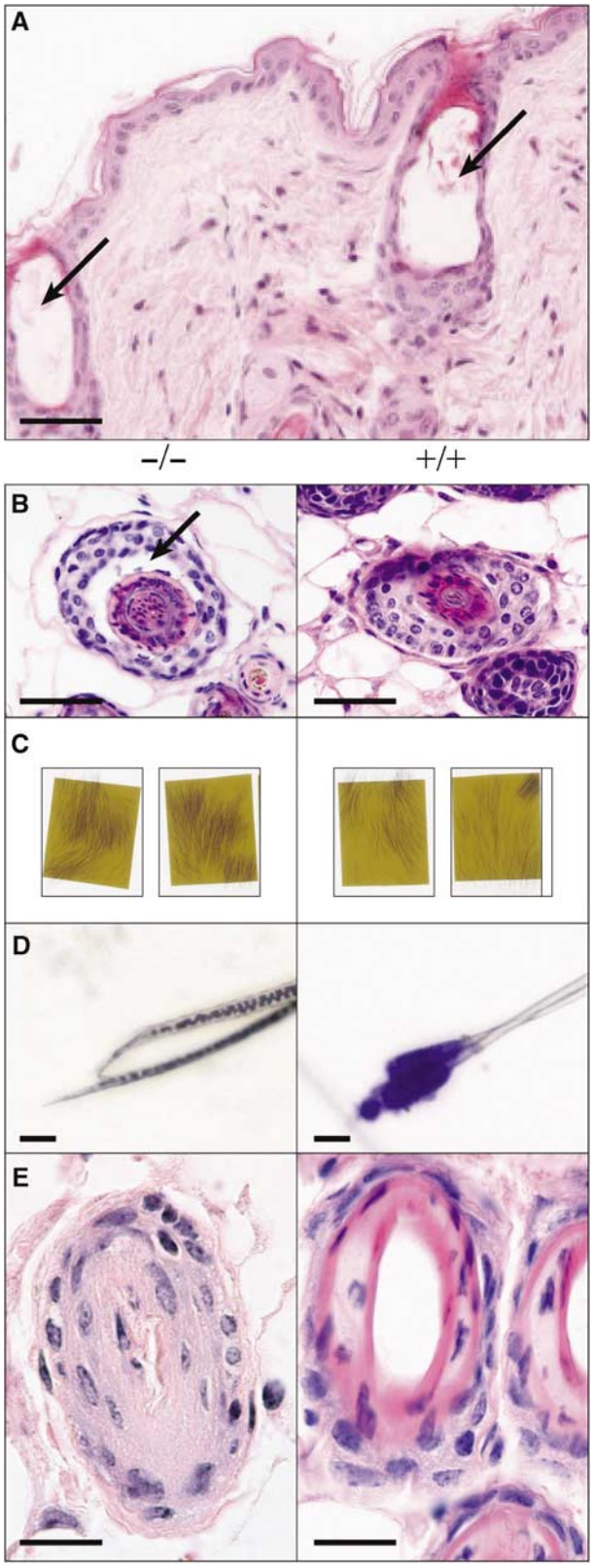

The formation of these clefts is due to shrinkage of the tissue caused by dehydration from the ethanol fixing. As shown in Figure 3B, cleft formation was evident between the IRS and ORS in *Grhl1*$^{-/-}$ mice, but not in wild-type littermate controls. We also examined hair anchorage using a tape-stripping test, in which adhesive tape was applied to the dorsal region of the trunk and peeled off in the direction of hair growth (Figure 3C; Koch *et al*, 1998). Despite the thinner hair covering of the *Grhl1*$^{-/-}$ mice, substantially more hair was lost from the mutant animals than their wild-type littermate controls. Hair numbers adherent to the tape per low power microscopic field varied between 400 and 500 in the mutant strain compared with 100–200 in the wild-type animals.

The rate of hair regrowth following depilation was identical in both wild-type and mutant mice (Supplementary Figure 6). Examination of depilated hairs removed during anagen revealed that the shafts remained intact, and had not broken at any point along the shaft. Toluidine blue staining of these hairs from wild-type and mutant mice uncovered a marked difference (Figure 3D). Adherent to the proximal tip of the wild-type hair was an intensely stained ball of tissue that consisted of the IRS, companion layer and ORS (Hanakawa *et al*, 2004). In contrast, the mutant hair displayed naked anagen hair bulbs lacking any of the usual tissue layers. This finding is reminiscent of the appearance of plucked anagen hairs in human patients with loose anagen hair syndrome (Baden *et al*, 1992). Consistent with this, we observed marked differences in the appearance of depilated follicles between wild-type and mutant mice, with retention of the IRS in the *Grhl1*-null animals (Figure 3E).

Defining the GRHL1 consensus DNA-binding site

The molecular events underlying the defects observed in the *Grhl1*-null hair follicles presumably reflected altered expression of target genes of this transcription factor. To date, the consensus DNA-binding sequence of this factor remained unknown. To address this, we initially performed cyclic amplification and selection of targets (CASTing) (Wright *et al*, 1991). For this purpose, we used cellular extracts from a human placental choriocarcinoma cell line JEG-3 that we had previously shown to contain abundant GRHL1 (see Materials and methods). We had successfully employed this strategy to define the consensus DNA-binding site for GRHL3 (Ting *et al*, 2005). After six cycles, the population of selected binding sites was cloned and individual isolates sequenced and aligned (Supplementary Figure 7). The defined GRHL1

Figure 3 Analysis of the epidermis and hair in adult *Grhl1*$^{-/-}$ mice. (**A**) Histology of the skin from a hypotrichotic area of a 4-month-old *Grhl1*-null mouse revealing cysts (arrows) in telogen follicles. (**B**) Histology of horizontal cross-sections of skin fixed with 70% ethanol from a 45-day-old *Grhl1*-null mouse (–/–) and wild-type (+/+) littermate control. Cleft formation between the IRS and ORS in the *Grhl1*-null sample is indicated by an arrow. (**C**) Loose anchoring of hair in the *Grhl1*$^{-/-}$ mice. Adhesive tape was applied to the dorsal skin of 2-month-old *Grhl1*-null mice (–/–) and their wild-type littermates (+/+). The tape was then gently pulled in the direction of hair growth. (**D**) Toluidine blue staining of anagen hair follicles extracted from a 45-day-old *Grhl1*-null mouse (–/–) and a wild-type littermate control (+/+). (**E**) Histology of horizontal cross-sections of depilated skin from a 45-day-old *Grhl1*$^{-/-}$ mouse and wild-type littermate control. The scale bars are equivalent to 100 μm in (A–E).

©2008 European Molecular Biology Organization

DNA-binding consensus sequence (AACCGGTT) was identical to that defined for GRHL3, and also matched the consensus sequence for *Drosophila* GRH DNA binding, which we had previously identified by alignment of multiple GRH-responsive gene regulatory regions (Wilanowski *et al*, 2002; Ting *et al*, 2005). Of note, the first of the two cytosines and the second of the guanines were invariant in both GRHL1 and GRHL3 CASTing assays.

Reduced expression of the Dsg1 genes in Grhl1-deficient mice

Our histological analyses, as well as analyses of others, suggested that defects in hair anchoring underpinned the *Grhl1*-deficient phenotype. Previous studies have implicated members of the desmosomal cadherin family in this process (Koch *et al*, 1998; Hanakawa *et al*, 2004), and this, coupled with the links between *grh* and cadherin family members in *Drosophila* prompted us to examine the potential role of these genes in the *Grhl1*-deficient mice.

The desmosomal cadherins are adhesion molecules that are critical components of the intercellular junctions in the epidermis, the desmosomes (Garrod *et al*, 2002; Yin and Green, 2004). The family consists of the desmocollins (*Dsc*) and *Dsgs*, each of which has multiple subtypes in mice and humans (*Dsg1–4* and *Dsc1–3*) that are expressed in a differentiation-dependent pattern (Garrod *et al*, 2002; Yin and Green, 2004). In addition, mice have three *Dsg1* isoforms (*Dsg1*α, *Dsg1*β, and *Dsg1*γ) (Kljuic and Christiano, 2003; Pulkkinen *et al*, 2003; Whittock, 2003), which exhibit varying expression patterns in the differentiating cell layers in the epidermis (Brennan *et al*, 2004). In the hair follicle, all three *Dsg1* isoforms are present, but are subject to significant hair cycle-dependent changes (Brennan *et al*, 2004). To determine whether the desmosomal cadherins were potential GRHL1 target genes, we surveyed the regulatory regions of these genes for potential GRHL1-binding sites. As shown in Figure 4A, the three mouse *Dsg1* genes and the human *DSG1* gene all contained a putative GRHL1-binding motif, with a conserved first cytosine and second guanine. The putative GRHL1-binding site in the human *DSG1* promoter was located 12–34 bp upstream of the four reported transcription start sites (Adams *et al*, 1998). Although the locations of the transcription start sites in the mouse *Dsg1* genes have not been reported, there is significant homology between the three mouse genes and the human gene in the promoter regions, suggesting that GRHL1-binding sites also reside in the proximal *Dsg1* promoters in the mouse. No GRHL1 consensus-binding sites were found in the human or mouse *Dsg2*, *Dsg3*, or *Dsg4* genes, or in any of the *Dsc* genes from these species (data not shown).

Our earlier RNA and reporter gene data (Figure 2) had demonstrated that *Grhl1* was expressed in the IRS of the hair follicle, a region also known to express the *Dsg1* genes (Brennan *et al*, 2004; Hanakawa *et al*, 2004). To confirm this at a protein level, and to visualize the coexpression of GRHL1 and DSG1, we performed immunohistochemistry on single sections of epidermis from wild-type mice using antisera to both proteins and the ImmPRESS multiple antigen labelling system (see Material and methods). GRHL1 and DSG1 were coexpressed in the IRS (Figure 4B) and the sebaceous glands (data not shown).

To ascertain whether the level or distribution pattern of DSG1 protein was altered in the *Grhl1*$^{-/-}$ animals, we performed immunohistochemistry on wild-type and mutant skin with antisera to DSG1 (Figure 4C). A marked reduction in protein expression was observed in both the hair follicles and interfollicular epidermis of the *Grhl1* mutants compared with the controls. We then performed northern analysis using RNA from skin with a probe that would hybridize to all three mouse *Dsg1* genes. We also examined the expression of *Dsg3*, which lacks a GRHL1-binding site in its regulatory regions, in these samples. As shown in Figure 4D, expression of *Dsg1* was specifically reduced in the mutant strain. Quantitation of the signals by densitometry revealed that *Dsg1* levels were threefold lower in the *Grhl1*-deficient skin. In contrast, the expression of *Dsg3* was not altered in the *Grhl1*-deficient skin. To confirm our northern analysis, and to investigate whether changes in expression of other cell adhesion genes may contribute to the observed phenotype, we studied the expression of *Dsg1*, *Dsg2*, *Dsg3*, *E-cadherin* (*Cdh1*), *P-cadherin* (*Cdh3*), *desmoplakin* (*Dsp*), and *desmocollin 1* (*Dsc1*) in the *Grhl1*-null mice by Q-RT–PCR (Figure 4E). *Dsg1* expression was significantly reduced in the *Grhl1*$^{-/-}$ epidermis. No significant differences in expression levels of the other genes were observed in the mutants compared with their wild-type littermates, with the exception of *Dsg2*, which was upregulated twofold in the mutant epidermis. The upregulation of *Dsg2* is unlikely to contribute significantly to the desmosomal cadherin protein pool, as the levels of DSG2 protein in adult skin are extremely low in normal adult skin (Mahoney *et al*, 2006). We also performed a microarray (Illumina) experiment, using epidermal-derived RNA from three wild-type and three mutant mice. We did not find any significant changes in the expression of cell adhesion genes in the *Grhl1*-knockout mice, consistent with the reduced sensitivity of this methodology as compared to Q-RT–PCR. A number of genes were found to be differentially expressed, but none of these have been linked to hair anchoring (data not shown).

To confirm the *Dsg1* genes as direct targets of GRHL1, we performed electrophoretic mobility shift assays (EMSA) (Figure 4F). The putative GRHL1-binding motif (GACTGGTT) is perfectly conserved, together with 6 bp upstream and 12 bp downstream flanking sequences, in three of the *Dsg1* promoters: mouse *Dsg1*α, mouse *Dsg1*γ, and human *DSG1* (Figure 4A). In the mouse *Dsg1*β promoter, this motif is slightly different (AACTGGTT), although the flanking sequences are still conserved. Consequently, we designed two probes for the EMSA, one derived from the human *DSG1* promoter, and the other based on the mouse *Dsg1*β promoter. Using nuclear extract derived from the JEG-3 cell line, we demonstrated several DNA/protein complexes with the mouse probe (lane 1). The upper band (arrowed) was specifically supershifted with the addition of anti-GRHL1 antisera (lane 2). This band was specific, as it was competed off with excess unlabelled mouse *Dsg1*β probe (lane 3). It was also competed off with excess unlabelled human *DSG1* probe (lane 4). The human *DSG1* probe revealed a less complex array of protein/DNA complexes, but the GRHL1 complex was retained (lane 5) and specifically supershifted with anti-GRHL1 antisera (lane 6). The GRHL1 band was also competed away with excess unlabelled, human *DSG1* (lane 7) and mouse *Dsg1*β probe (lane 8), indicating that GRHL1 binds specifically to the *Dsg1* promoters in mice and humans.

 ©2008 European Molecular Biology Organization

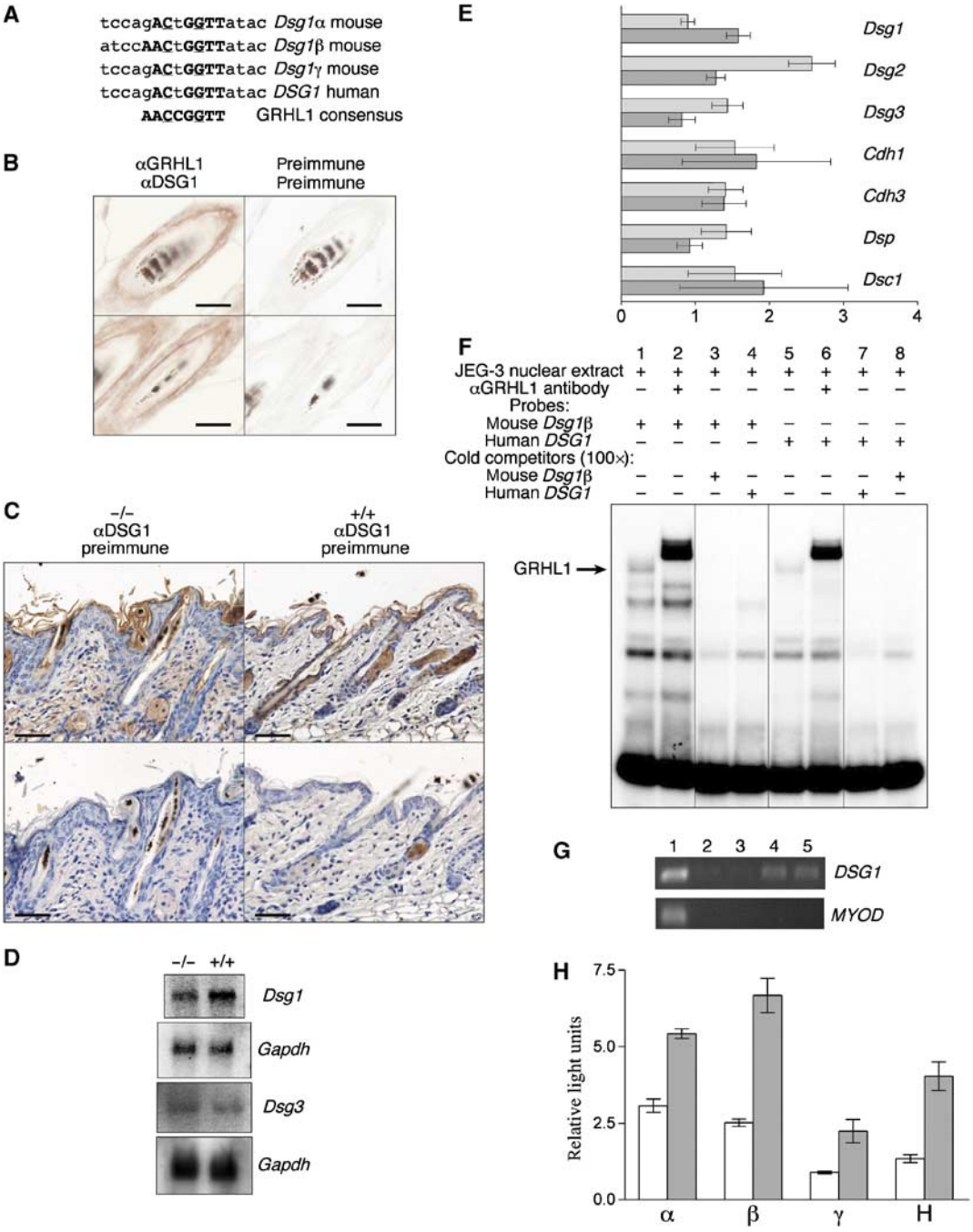

Figure 4 Mouse and human *Dsg1* genes are direct targets of GRHL1 regulation. (**A**) Alignment of the promoter regions of *Dsg1* genes from mouse and human to the consensus DNA-binding sequence for GRHL1. Conserved bases are bolded and the invariant cytosine and guanine are underlined. Sequences of *Dsg1* promoters were obtained from the GenBank database, entries AC108943 (*Dsg1*α and *Dsg1*γ, AC102410 (*Dsg1*β, and AC009717 (human *DSG1*. (**B**) Immunohistochemistry of DSG1 and GRHL1 in wild-type mouse skin. Polyclonal antisera to mouse DSG1 was added first and developed with NovaRed (red colour). After re-blocking with horse serum, polyclonal antisera to mouse GRHL1 was added and developed with DAB-Ni (gray/black colour) (left panels). Adjacent sections exposed to the respective pre-immune sera (right panels). (**C**) Immunohistochemistry of DSG1 expression in *Grhl1*$^{-/-}$ and *Grhl1*$^{+/+}$ skins. Top panels: anti-DSG1 antibody; bottom panels: pre-immune sera. The scale bars are equivalent to 500 μm. (**D**) Northern analysis of *Dsg1* and *Dsg3* mRNA expression in the skin from *Grhl1*-null and wild-type mice. The *Gapdh* probe served as the loading control. (**E**) Quantitative RT–PCR analysis of epidermal RNA from *Grhl1*-null and wild-type mice. *Grhl1*$^{-/-}$ samples are shown as lighter boxes and wild-type controls as darker boxes. Bars represent standard errors. The *HPRT* levels served as reference. (**F**) DNA binding of GRHL1. Extract from the JEG-3 cell line was studied with the probes from the mouse *Dsg1*β and human *DSG1* promoters. A 100-fold molar excess of unlabelled cold competitor probe was added in the indicated lanes. The αGRHL1 antibody 67 was added where indicated. The migration of the specific GRHL1/DNA complex is arrowed. (**G**) Binding of GRHL1 to the human *DSG1* promoter demonstrated by ChIP assay. Chromatin from HaCaT cells was immunoprecipitated using two different antisera to GRHL1, 67 (lane 4) and 611 (lane 5). As negative controls, we used pre-immune sera (lane 3) and no added sera (lane 2). Lane 1 shows the input chromatin. The immunoprecipitated chromatin was amplified with *DSG1* or the control *MYOD* primers. (**H**) GRHL1 transactivates *Dsg1* promoters. 293T cells were transiently cotransfected with the proximal promoters of the mouse (*Dsg1*α, β and γ) and human *DSG1* (H) genes linked to the firefly luciferase reporter gene with an expression vector containing the *Grhl1* cDNA (shaded bars) or the vector alone (open bars). Each experiment was performed in triplicate. Bars indicate the standard deviations.

©2008 European Molecular Biology Organization

To confirm this binding in an *in vivo* setting, we performed chromatin immunoprecipitation (ChIP) using the human keratinocyte cell line, HaCaT (Figure 4G). We initially determined by RT–PCR that both *GRHL1* and *DSG1* are expressed in this cell line (data not shown). Crosslinked protein/chromatin complexes were immunoprecipitated with two different anti-GRHL1 antisera (lanes 4 and 5), and after reversal of the crosslinking the precipitates were subjected to PCR with primers flanking the GRHL1-binding site in the *DSG1* promoter (upper panel). The promoter from the *MYOD* gene (which is not expressed in these cells) was used as a negative control (lower panel) (Sawado *et al*, 2001). Pre-immune sera from one of the GRHL1 immunized rabbits (lane 3) and no sera (lane 2) served as additional controls. Occupancy of the *DSG1* promoter by GRHL1 was evident in this cell line. The input chromatin for each experiment is shown in lane 1.

We also performed reporter gene assays with the individual mouse and human *Dsg1* promoters in the setting of enforced *Grhl1* expression (Figure 4H). The human embryonic kidney cell line 293T was cotransfected with the individual human and mouse *Dsg1* promoters linked to the firefly luciferase gene and a mammalian expression vector carrying the mouse *Grhl1* gene. An empty vector was transfected with the reporter constructs as a control, and transfection efficiency was established with a plasmid expressing Renilla luciferase. All four promoters were *trans*-activated to varying extents by *Grhl1* in this context, consistent with the reduction in *Dsg1* expression observed in the *Grhl1*-deficient mice. We then examined the effect of mutating the nearly optimal GRHL1-binding site in the Dsg1 promoter and found that loss of this site in isolation did not ablate GRHL1-dependent activation (data not shown). We reexamined the region of the promoter that we identified by ChIP to contain the GRHL1-binding site(s) and, eventually, identified two other sites matching the binding sequences previously identified in our CASTing assay, which were also conserved in the human *DSG1* promoter. This suggests, as with many other transcription factors, that multiple binding sites are present in key regulatory regions. To investigate the specificity of the response to GRHL1, we examined whether the *Dsg1* promoter was also responsive to GRHL3 in transfection experiments (Supplementary Figure 8). Despite the fact that GRHL1 and GRHL3 have identical *in vitro*-defined DNA-binding consensus sequences, GRHL3 was unable to activate the *Dsg1* promoter.

Grhl1-null mice exhibit palmoplantar keratoderma

In humans, mutations in the *DSG1* gene result in the dominantly inherited disorder striate PPK (SPPK), typified by hyperkeratosis at sites of pressure and abrasion, the palms, and soles (Rickman *et al*, 1999; Hunt *et al*, 2001). Histological examination of the palmopalmar surface of the paws of the *Grhl1*-null mice revealed marked thickening of the stratum corneum, consistent with PPK (Figure 5A). Analysis of expression of different keratins in humans with DSG1-SPPK revealed a reduction of K5 and K14, with weak staining of K10 remaining in the lower suprabasal layers (Wan *et al*, 2004). Studies in the *Grhl1*-mutant mice also revealed a marked reduction in K14 expression and a less dramatic reduction in K5 expression compared with wild-type controls (Figure 5B and C). Expression of K10 was also altered, with weak staining confined to the upper spinous and granular layers (Figure 5D). However, the levels of involucrin, a differentiation marker, were decreased (Figure 5E), which was inconsistent with DSG1-SPPK patient data (Wan *et al*, 2004).

Ultrastructural studies of the interfollicular epidermis unveiled more abnormalities in the *Grhl1*-null mice (Figure 5F). Fewer desmosomes were identifiable (Table I), and these appeared to be shorter and less well organized (Figure 5F). We then examined desmosomal number in cultured wild-type and mutant epidermis following treatment with EGTA, which has no effect on normal epidermis, but induces dissociation in the setting of desmosomal instability (Garrod *et al*, 2005). Consistent with our other findings, EGTA treatment led to a further reduction in desmosomal number (Table I).

Discussion

Many cellular functions require stringent control of attachment to, and detachment from, other cells or biological surfaces. An example of dynamic adhesive interactions is anchoring of the hair shaft to the hair follicle, in which the desmosomal cadherins have a pivotal role. The studies reported here implicate the transcription factor *Grhl1* in the regulation of hair anchoring and reveal a direct link between this factor and the human and mouse *Dsg1* genes. Expression of *Grhl1* in the mouse hair follicle was observed in the IRS of the follicle, but not in the dermal papilla cells, mirroring the pattern of expression of the *Dsg1* genes (Brennan *et al*, 2004). Mice deficient in *Grhl1* showed a delay in the appearance of their coat, sporadic regional hair loss, and excess hair loss with tape stripping and abnormal clefting between the IRS and ORS, which are the features of loss of *Dsg1* expression (Hanakawa *et al*, 2004). Northern blotting and Q-RT–PCR confirmed that the levels of *Dsg1* were reduced in the mutant mice compared with wild-type littermate controls. Sequence analysis, DNA binding, and ChIP experiments demonstrated that the mouse and human *Dsg1* promoters were direct targets of GRHL1, and transfection assays confirmed the ability of GRHL1 to activate these regulatory elements. These findings suggest that GRHL1 is an important regulator of the *Dsg1* genes in the context of mammalian hair anchorage.

Studies of mice carrying mutations in the desmosomal cadherin genes have illustrated the role of this family in the growth and anchoring of the hair follicle (Garrod *et al*, 2002). Mice carrying a targeted deletion of the *Dsg3* gene show normal follicular neogenesis, and then develop defective hair anchoring in the quiescent (telogen) phase of the growth cycle (Koch *et al*, 1998). These animals also exhibit a skin phenotype that resembles pemphigus vulgaris (Koch *et al*, 1997). Mice deficient in *Dsc1* and *Dsg4* also exhibit skin and hair phenotypes, although defective hair anchorage is not a feature of these mutants (Chidgey *et al*, 2001; Kljuic *et al*, 2003). Mutations in the *desmoplakin* and *plakoglobin* genes manifest with PPK, hair abnormalities, and cardiomyopathy (McGrath, 2005). The hair phenotype in these patients is described as 'woolly', and as such does not resemble the anchorage defects seen in the *Grhl1*-null mice. Histological examination of the heart from the *Grhl1* mutant mice revealed no evidence of cardiomyopathy (data not shown). The presence of three *Dsg1* genes in mice has presumably precluded their inactivation by standard gene targeting. Instead, inactivation of two of the DSG1 isoforms (DSG1α and DSG1β) by a serine protease produced by *Staphylococcus aureus*,

 ©2008 European Molecular Biology Organization

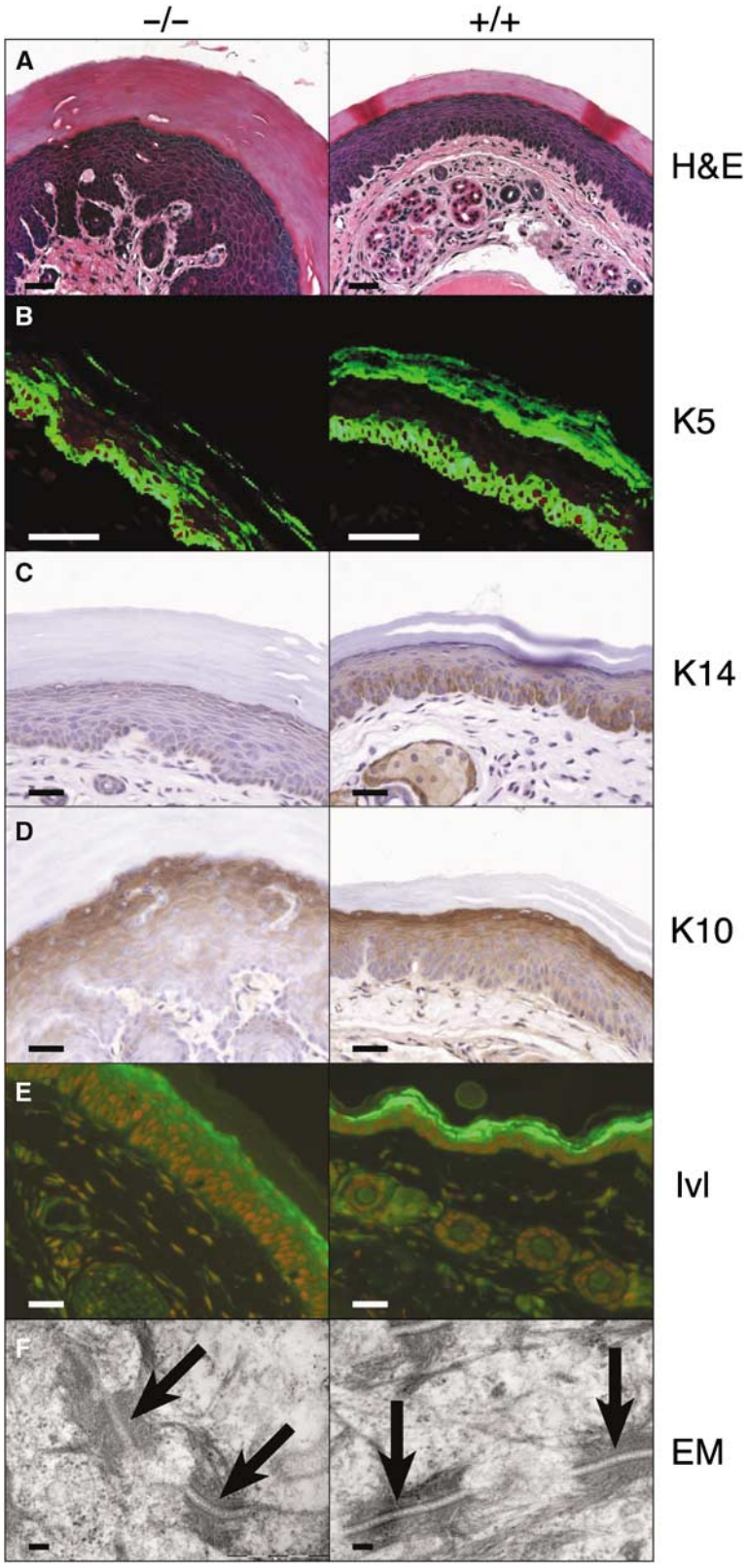

Figure 5 *Grhl1*-null mice exhibit features of PPK. (**A**) Histology of the palmar surface of the forepaw of a *Grhl1*-null (−/−) and wild-type (+/+) littermate at 7 months of age. (**B**–**E**) Immunohistochemistry (C, D) or immunofluorescence (B, E) of keratin and involucrin expression in palmar sections from 7 months old $Grhl1^{-/-}$ and $Grhl1^{+/+}$ mice. The staining was performed with antisera against K5 (B), K14 (C), K10 (D), and involucrin (E). (**F**) Transmission electron microscopy of interfollicular epidermis. Arrows point to individual desmosomes. The scale bars are equivalent to 100 μm in (A–E) and 100 nm in (F).

©2008 European Molecular Biology Organization

Table I Comparison of desmosome numbers in *Grhl1*$^{+/+}$ and *Grhl1*$^{-/-}$ epidermis untreated or treated with EGTA

Sample 1	Sample 2	Mean difference per field	s.e.	Significance[#]
Grhl$^{+/+}$ untreated	Grhl$^{-/-}$ untreated	−3.05714	0.96105	0.023
Grhl$^{+/+}$ −EGTA	Grhl$^{+/+}$ + EGTA	−0.35000	0.97270	0.999
Grhl$^{-/-}$ −EGTA	Grhl$^{-/-}$ + EGTA	−2.96111	0.99936	0.042

[#]Statistical analysis was performed using Tukey HSD *post hoc* test with $P<0.05$ considered significant.

exfoliative toxin A (ETA) in the setting of *Dsg3* deficiency has been examined (Hanakawa *et al*, 2004). These mice exhibited a specific loss of anagen hair with tape stripping and separation between the ORS and IRS of the hair follicle, a histological feature we also observed in the *Grhl1*-deficient mice. In contrast, ETA-induced loss of these DSG1 isoforms in the setting of wild-type levels of DSG3 did not lead to defective hair anchoring or histological abnormalities, suggesting that DSG3 can compensate for loss of DSG1α and DSG1β. Our data suggest that DSG1γ, the ETA-resistant isoform of DSG1 (Brennan *et al*, 2004), also has a key role in this compensation, as reduced total *Dsg1* expression in *Grhl1*-deficient mice in the setting of wild-type levels of *Dsg3* leads to severe hair anchoring defects. *Dsg1*γ is highly expressed in the IRS of the lower hair follicle and in the sebaceous glands, analogous to *Grhl1*, and the *Dsg1*γ promoter contains a GRHL1 consensus site. Computational analyses suggest that the very low hydrophilic potential of the extracellular anchoring domain of DSG1γ may provide it with a stronger affinity for the cell membrane than the other DSG1 isoforms, underpinning its potential importance in hair shaft anchoring (Brennan *et al*, 2004).

The phenotype induced by the *Grhl1*-mediated reduction in total *Dsg1* levels is unlike the ETA-treated *Dsg3*-null mice in that it manifests as poor hair anchorage at all stages of the hair cycle, not just in anagen. This was evident in our tape-stripping experiments, in which hair was readily removed irrespective of the growth cycle stage, and in the histological identification of empty dilated telogen hair follicles, reminiscent of the mice carrying a targeted deletion of the *Dsg3* gene. We suspect that the delay in initial hair appearance was contributed to by maternal grooming, as hair growth improved at the time of weaning, while hair loss in young pups was variable between litters, but consistent within the same litter. Also commensurate with this, older mice showed sporadic regional hair loss, which was not observed when animals were housed in isolation. Although it is possible that the phenotypic variability observed was also influenced by modifier loci, these have not been described in the context of other depilation defects.

In addition to hair anchorage defects, the *Grhl1*-null mice exhibited keratoderma of the palmar surface of the front-paws and the plantar surface of the hind-paws accompanied by disordered expression of keratins 5, 10, and 14, a phenotype mimicking the appearance of SPKK in patients with *DSG1* mutations. The expression of involucrin was decreased, which is in contrast to patients with SPPK, indicating that subtle species differences exist in this condition. Hair disorders have also not been reported in these patients, and we postulate that this may be due to a dosage effect, as *DSG1* mutations in humans result in haploinsufficiency, with proteins levels predicted to be at 50% of normal. The lack of skin or hair phenotypes in the *Grhl1*$^{+/-}$ animals is not surprising, as these mice presumably exhibit much higher levels of *Dsg1* expression than homozygous *Grhl1*$^{-/-}$ mutants.

Accumulating evidence suggests that the specific distribution pattern of desmosomal proteins is not merely a result of differentiation, but may in fact drive tissue morphogenesis and function (Green and Gaudry, 2000). Despite this, little is known about the spatio-temporal transcriptional regulation of desmosomal components. C/EBP transcription factors have been shown to regulate the expression of desmocollin genes, but not Dsgs (Smith *et al*, 2004). A region 4.2 kb 5′ of the transcription start site in the human *DSG1* promoter is sufficient to confer expression in the epidermis and hair follicles (Adams *et al*, 1998). This region encompasses the GRHL1-binding site. In addition, protein kinase C (PKC) has been shown to positively regulate *DSG1*, with little effects on the other *DSG* genes (Denning *et al*, 1998). Although we are yet to establish whether PKC signalling acts through *Grhl1*, this pathway has been linked to the *Grhl* family in the context of neural tube closure, as demonstrated in the curly tail mice, which carry a mutation in the *Grhl3* gene (Ting *et al*, 2003a; Cogram *et al*, 2004). Our data suggest that hair anchorage is sensitive to the absolute levels of *Dsg* expression. Consistent with this, a two- to threefold elevation in *Dsg1* and *Dsg3* levels in the plucked (*pk*) mutant mouse leads to impaired hair growth with retention of IRS in the follicle (Luo *et al*, 2005), and altered patterns of expression of individual Dsgs perturb epidermal differentiation (Elias *et al*, 2001; Merritt *et al*, 2002). These observations highlight the need for precise regulation of *Dsg* expression in the hair follicle.

Disruptions of DSG1 protein function can also result in cell–cell dis-adhesion and blistering in the superficial epidermis (Anhalt *et al*, 1982; Udey and Stanley, 1999; Amagai *et al*, 2000; Hanakawa *et al*, 2002). The *Grhl1*-deficient mice did not exhibit a blistering phenotype, although we observed desmosomal defects in the interfollicular epidermis, which had fewer desmosomes than controls. These desmosomes were shorter, less-organized, and weakly adhesive, as demonstrated by their sensitivity to EGTA treatment (Garrod *et al*, 2005). However, this desmosomal phenotype was not sufficiently severe to cause skin blistering. Consistent with this, the Nikolsky test for epidermal fragility was negative (data not shown) (Polifka and Krusinski, 1980). We conclude that there were sufficient desmosomes present in the *Grhl1*$^{-/-}$ epidermis to prevent skin blistering.

Our studies expand the functional comparisons between *Drosophila grh* and the mammalian *Grhl* genes that were initially examined in the context of formation and repair of the epidermal barrier (Ting *et al*, 2005). The consensus DNA-binding sequence identified for GRHL1 is identical to that defined for *Drosophila* GRH (Wilanowski *et al*, 2002). In addition, the identification of cadherin genes as direct transcriptional targets of GRHL1 extends the links between the

 ©2008 European Molecular Biology Organization

grh and cadherin gene families from *Drosophila* to mammals. The cadherin family consists of more than 100 members (including the protocadherins) involved in many diverse cellular and developmental events (Nollet *et al*, 2000). Among the known targets of *Drosophila*, GRH are two cadherin superfamily members, *stan/fmi* and *E-cadherin/shotgun* (Lee and Adler, 2004; Almeida and Bray, 2005). The links between the two gene families have recently been extended in another model organism. A study of genome-wide predictions of genetic interactions in *C. elegans* has identified a number of cadherin family members as prime targets for significant functional interactions with *Grh-1*, the worm homologue of *grh* (Zhong and Sternberg, 2006). These included *cdh-6*, a homologue of *Drosophila stan*, and *hmp-2*, a β-catenin. We have recently identified the mammalian homologue of *E-cadherin* as a target of another member of the *Grh*-like family, *Grhl2* (JMC and SMJ, unpublished). Our ongoing studies will examine their functional relevance.

The ablation of *Grhl1* expression does not completely inactivate the *Dsg1* genes, suggesting that there are other factors involved in their regulation. Also, the *Grhl1* gene is expressed in many tissues that do not express *Dsg1*, and the apparent lack of phenotype associated with these tissues may be due to compensation from other *Grhl* family members. To this end, we have generated mice carrying mutations at both *Grhl1* and *Grhl3* loci. Mice null for both *Grhl1* and *Grhl3* died at birth, with neural tube defects that were identical to those observed in *Grhl3*-null embryos. $Grhl1^{-/-}Grhl3^{+/-}$ animals did not show any differences in phenotype to that observed with loss of *Grhl1* alone. It is unclear whether the residual *Grhl3* allele is sufficient to partially compensate for the loss of *Grhl1*, or compensation is provided by another factor. Our transfection data suggest that GRHL3 is incapable of activating the *Dsg1* promoter, suggesting that it may have no role in this context. The development of a conditional *Grhl3* allele will allow this question to be addressed further.

Materials and methods

Microscopy, digital photography, and image processing

Gross images were obtained using a digital camera (Fuji FinePix S2 Pro with 60 mm Micro Nikon lens) or a dissection microscope (model SMZ-U, Nikon) equipped with a camera (AxioCam, Zeiss) driven by AxioVision (Zeiss). Microscopy images were obtained using a microscope (Optiphot-2, Nikon) and the same camera.

EMSA

This assay was carried out according to the previously published protocol, using the same nuclear extract and antibodies (Wilanowski *et al*, 2002). Two oligonucleotide probes were used (sense strand only given): human *Dsg1* promoter 5′-GGTGGGGAT CCAGACTGGTTATACGTACCTTC-3′, mouse *Dsg1*β promoter 5′-GGGTGGAGATCCAACTGGTTATACGTACCTTC-3′.

Luciferase reporter gene activity assay

Luciferase activity assays employed the dual-luciferase reporter assay system (Promega). Promoter elements from the mouse and human *Dsg1* genes were PCR amplified and cloned into *Kpn*I-*Xho*I cloning sites of the pGL3-Basic vector. The PCR primers introduced the required *Kpn*I and *Xho*I restriction sites at the ends of the amplification products. The primer sequences are included in the Supplementary data. For expression of *Grhl1*, the full-length mouse *Grhl1* cDNA (Wilanowski *et al*, 2002) was cloned into the pCAGGS vector. 293T cells were transiently cotransfected with the approximately 1 kb fragments of proximal promoters of the mouse and human *Dsg1* promoters linked to the firefly luciferase reporter gene, and either the empty pCAGGS vector or the pCAGGS vector containing the *Grhl1* cDNA. Cotransfection with the pTK-RL plasmid expressing Renilla luciferase served as the control of transfection efficiency. The results were standardized using Renilla luciferase assay. Each experiment was undertaken in triplicate.

Other experimental procedures

RT–PCR, Q-RT–PCR, histology, *in situ* hybridization, β-galactosidase staining, and electron microscopy were carried out as described (Wilanowski *et al*, 2002; Ting *et al*, 2003a, b; Wan *et al*, 2004; Majewski *et al*, 2006). Primer sequences are included in the Supplementary data. Desmosomal counts were obtained using two different methodologies. In the first, images were taken randomly, with the only criterion being that the cornified layer appeared in the image, and all images were captured at 25 K. In the second, images were taken side-by-side all at 25 K and were rotated so that the cornified layer lay parallel to one of the long axes. Twenty to 24 images were taken per section.

The CASTing assay was performed as described previously (Ting *et al*, 2005), except nuclear extract from JEG-3 cells, and anti-GRHL1 antibody no. 67 was used (Wilanowski *et al*, 2002). Northern blots were performed as described previously (Ting *et al*, 2005). The *Dsg1*-specific probe encompassed nt 1808–2405 (GenBank entry AK036986), a region common to all three *Dsg1* isoforms. The *Dsg3*-specific probe encompassed nt 1162–1822 (GenBank entry NM_030596). Signal strengths were quantified using PhosphorImager, driven by ImageQuant 5.0 (Molecular Dynamics).

The ChIP experiment followed the published protocol (Forsberg *et al*, 2000).
Primers specific for the human *DSG1* promoter were:
forward, 5′-CCCTCGGTATTTCTGTTCAC-3′
reverse, 5′-CATCCAAGACCAAGGGAGTT-3′
Primers specific for the *MYOD* promoter were used as negative control (Zhao *et al*, 2004).

Immunohistochemistry on single sections of wild-type mouse skin was performed using the ImmPRESS multiple antigen labelling system as per the manufacturer's instructions (Vector Laboratories, Burlingame, CA). Polyclonal antisera to mouse DSG1 was added first and developed with NovaRed (red colour). After re-blocking with horse serum, polyclonal antisera to mouse GRHL1 was added and developed with DAB-Ni (gray/black colour).

Supplementary data

Supplementary data are available at *The EMBO Journal* Online (http://www.embojournal.org).

Acknowledgements

We thank members of the Jane lab, Walt Holleran, and Peter Elias for helpful discussions; S Hunjan and Ozgene Inc. (Perth, Australia) for technical assistance; and John Stanley for the kind gift of DSG1 and DSG3 antisera. Animal support was provided by staff from the Walter & Eliza Hall Institute. SMJ is a Principal Research Fellow of the Australian National Health and Medical Research Council (NHMRC). This work was supported by Grants from the Australian NHMRC and The March of Dimes Foundation.

References

Adams MJ, Reichel MB, King IA, Marsden MD, Greenwood MD, Thirlwell H, Arnemann J, Buxton RS, Ali RR (1998) Characterization of the regulatory regions in the human desmoglein genes encoding the pemphigus foliaceous and pemphigus vulgaris antigens. *Biochem J* **329:** 165–174

Almeida MS, Bray SJ (2005) Regulation of post-embryonic neuroblasts by *Drosophila* Grainyhead. *Mech Dev* **122:** 1282–1293

Amagai M, Matsuyoshi N, Wang ZH, Andl C, Stanley JR (2000) Toxin in bullous impetigo and staphylococcal scalded-skin syndrome targets desmoglein 1. *Nat Med* **6:** 1275–1277

©2008 European Molecular Biology Organization

Anhalt GJ, Labib RS, Voorhees JJ, Beals TF, Diaz LA (1982) Induction of pemphigus in neonatal mice by passive transfer of IgG from patients with the disease. *N Engl J Med* **306:** 1189–1196

Auden A, Caddy J, Wilanowski T, Ting SB, Cunningham JM, Jane SM (2006) Spatial and temporal expression of the Grainyhead-like transcription factor family during murine development. *Gene Expr Patterns* **6:** 964–970

Baden HP, Kvedar JC, Magro CM (1992) Loose anagen hair as a cause of hereditary hair loss in children. *Arch Dermatol* **128:** 1349–1353

Bray SJ, Kafatos FC (1991) Developmental function of Elf-1: an essential transcription factor during embryogenesis in *Drosophila*. *Genes Dev* **5:** 1672–1683

Brennan D, Hu Y, Kljuic A, Choi Y, Joubeh S, Bashkin M, Wahl J, Fertala A, Pulkkinen L, Uitto J, Christiano AM, Panteleyev A, Mahoney MG (2004) Differential structural properties and expression patterns suggest functional significance for multiple mouse desmoglein 1 isoforms. *Differentiation* **72:** 434–449

Chidgey M, Brakebusch C, Gustafsson E, Cruchley A, Hail C, Kirk S, Merritt A, North A, Tselepis C, Hewitt J, Byrne C, Fassler R, Garrod D (2001) Mice lacking desmocollin 1 show epidermal fragility accompanied by barrier defects and abnormal differentiation. *J Cell Biol* **155:** 821–832

Cogram P, Hynes A, Dunlevy LP, Greene ND, Copp AJ (2004) Specific isoforms of protein kinase C are essential for prevention of folate-resistant neural tube defects by inositol. *Hum Mol Genet* **13:** 7–14

Denning MF, Guy SG, Ellerbroek SM, Norvell SM, Kowalczyk AP, Green KJ (1998) The expression of desmoglein isoforms in cultured human keratinocytes is regulated by calcium, serum, and protein kinase C. *Exp Cell Res* **239:** 50–59

Elias PM, Matsuyoshi N, Wu H, Lin C, Wang ZH, Brown BE, Stanley JR (2001) Desmoglein isoform distribution affects stratum corneum structure and function. *J Cell Biol* **153:** 243–249

Forsberg EC, Downs KM, Bresnick EH (2000) Direct interaction of NF-E2 with hypersensitive site 2 of the beta-globin locus control region in living cells. *Blood* **96:** 334–339

Garrod DR, Berika MY, Bardsley WF, Holmes D, Tabernero L (2005) Hyper-adhesion in desmosomes: its regulation in wound healing and possible relationship to cadherin crystal structure. *J Cell Sci* **118:** 5743–5754

Garrod DR, Merritt AJ, Nie Z (2002) Desmosomal cadherins. *Curr Opin Cell Biol* **14:** 537–545

Green KJ, Gaudry CA (2000) Are desmosomes more than tethers for intermediate filaments? *Nat Rev Mol Cell Biol* **1:** 208–216.

Hanakawa Y, Li H, Lin C, Stanley JR, Cotsarelis G (2004) Desmogleins 1 and 3 in the companion layer anchor mouse anagen hair to the follicle. *J Invest Dermatol* **123:** 817–822

Hanakawa Y, Matsuyoshi N, Stanley JR (2002) Expression of desmoglein 1 compensates for genetic loss of desmoglein 3 in keratinocyte adhesion. *J Invest Dermatol* **119:** 27–31

Hunt DM, Rickman L, Whittock NV, Eady RA, Simrak D, Dopping-Hepenstal PJ, Stevens HP, Armstrong DK, Hennies HC, Kuster W, Hughes AE, Arnemann J, Leigh IM, McGrath JA, Kelsell DP, Buxton RS (2001) Spectrum of dominant mutations in the desmosomal cadherin desmoglein 1, causing the skin disease striate palmoplantar keratoderma. *Eur J Hum Genet* **9:** 197–203

Jane SM, Ting SB, Cunningham JM (2005) Epidermal impermeable barriers in mouse and fly. *Curr Opin Genet Dev* **15:** 447–453

Kljuic A, Bazzi H, Sundberg JP, Martinez-Mir A, O'Shaughnessy R, Mahoney MG, Levy M, Montagutelli X, Ahmad W, Aita VM, Gordon D, Uitto J, Whiting D, Ott J, Fischer S, Gilliam TC, Jahoda CA, Morris RJ, Panteleyev AA, Nguyen VT *et al* (2003) Desmoglein 4 in hair follicle differentiation and epidermal adhesion: evidence from inherited hypotrichosis and acquired pemphigus vulgaris. *Cell* **113:** 249–260

Kljuic A, Christiano AM (2003) A novel mouse desmosomal cadherin family member, desmoglein 1 gamma. *Exp Dermatol* **12:** 20–29

Koch PJ, Mahoney MG, Cotsarelis G, Rothenberger K, Lavker RM, Stanley JR (1998) Desmoglein 3 anchors telogen hair in the follicle. *J Cell Sci* **111:** 2529–2537

Koch PJ, Mahoney MG, Ishikawa H, Pulkkinen L, Uitto J, Shultz L, Murphy GF, Whitaker-Menezes D, Stanley JR (1997) Targeted disruption of the pemphigus vulgaris antigen (desmoglein 3) gene in mice causes loss of keratinocyte cell adhesion with a phenotype similar to pemphigus vulgaris. *J Cell Biol* **137:** 1091–1102

Lee H, Adler PN (2004) The grainy head transcription factor is essential for the function of the frizzled pathway in the *Drosophila* wing. *Mech Dev* **121:** 37–49

Luo J, Zhang L, Stenn K, Prouty S, Parimoo S (2005) Desmoglein genes are up-regulated in the pk mutant mouse. *Biochem Biophys Res Commun* **327:** 64–69

Mace KA, Pearson JC, McGinnis W (2005) An epidermal barrier wound repair pathway in Drosophila is mediated by grainy head. *Science* **308:** 381–385

Mahoney MG, Hu Y, Brennan D, Bazzi H, Christiano AM, Wahl JK (2006) Delineation of diversified desmoglein distribution in stratified squamous epithelia: implications in diseases. *Exp Dermatol* **15:** 101–109

Majewski IJ, Metcalf D, Mielke LA, Krebs DL, Ellis S, Carpinelli MR, Mifsud S, Di Rago L, Corbin J, Nicola NA, Hilton DJ, Alexander WS (2006) A mutation in the translation initiation codon of Gata-1 disrupts megakaryocyte maturation and causes thrombocytopenia. *Proc Natl Acad Sci USA* **103:** 14146–14151

McGrath JA (2005) Inherited disorders of desmosomes. *Australas J Dermatol* **46:** 221–229

Merritt AJ, Berika MY, Zhai W, Kirk SE, Ji B, Hardman MJ, Garrod DR (2002) Suprabasal desmoglein 3 expression in the epidermis of transgenic mice results in hyperproliferation and abnormal differentiation. *Mol Cell Biol* **22:** 5846–5858

Nollet F, Kools P, van Roy F (2000) Phylogenetic analysis of the cadherin superfamily allows identification of six major subfamilies besides several solitary members. *J Mol Biol* **299:** 551–572

Polifka M, Krusinski PA (1980) The Nikolsky sign. *Cutis* **26:** 521–525, 526

Pulkkinen L, Choi YW, Kljuic A, Uitto J, Mahoney MG (2003) Novel member of the mouse desmoglein gene family: Dsg1-beta. *Exp Dermatol* **12:** 11–19

Rickman L, Simrak D, Stevens HP, Hunt DM, King IA, Bryant SP, Eady RA, Leigh IM, Arnemann J, Magee AI, Kelsell DP, Buxton RS (1999) N-terminal deletion in a desmosomal cadherin causes the autosomal dominant skin disease striate palmoplantar keratoderma. *Hum Mol Genet* **8:** 971–976

Sawado T, Igarashi K, Groudine M (2001) Activation of beta -major globin gene transcription is associated with recruitment of NF-E2 to the beta-globin LCR and gene promoter. *Proc Natl Acad Sci USA* **21:** 21

Smith C, Zhu K, Merritt A, Picton R, Youngs D, Garrod D, Chidgey M (2004) Regulation of desmocollin gene expression in the epidermis: CCAAT/enhancer-binding proteins modulate early and late events in keratinocyte differentiation. *Biochem J* **380:** 757–765

Ting SB, Caddy J, Hislop N, Wilanowski T, Auden A, Zhao LL, Ellis S, Kaur P, Uchida Y, Holleran WM, Elias PM, Cunningham JM, Jane SM (2005) A homolog of *Drosophila* grainy head is essential for epidermal integrity in mice. *Science* **308:** 411–413

Ting SB, Wilanowski T, Auden A, Hall M, Voss AK, Thomas T, Parekh V, Cunningham JM, Jane SM (2003a) Inositol- and folate-resistant neural tube defects in mice lacking the epithelial-specific factor Grhl-3. *Nat Med* **9:** 1513–1519

Ting SB, Wilanowski T, Cerruti L, Zhao LL, Cunningham JM, Jane SM (2003b) The identification and characterization of human Sister-of-Mammalian Grainyhead (SOM) expands the grainyhead-like family of developmental transcription factors. *Biochem J* **370:** 953–962

Udey MC, Stanley JR (1999) Pemphigus—diseases of antidesmosomal autoimmunity. *JAMA* **282:** 572–576

Wan H, Dopping-Hepenstal PJ, Gratian MJ, Stone MG, Zhu G, Purkis PE, South AP, Keane F, Armstrong DK, Buxton RS, McGrath JA, Eady RA (2004) Striate palmoplantar keratoderma arising from desmoplakin and desmoglein 1 mutations is associated with contrasting perturbations of desmosomes and the keratin filament network. *Br J Dermatol* **150:** 878–891

Whittock NV (2003) Genomic sequence analysis of the mouse desmoglein cluster reveals evidence for six distinct genes: characterization of mouse DSG4, DSG5, and DSG6. *J Invest Dermatol* **120:** 970–980

Wilanowski T, Tuckfield A, Cerruti L, O'Connell S, Saint R, Parekh V, Tao J, Cunningham JM, Jane SM (2002) A highly conserved

 ©2008 European Molecular Biology Organization

novel family of mammalian developmental transcription factors related to *Drosophila* grainyhead. *Mech Dev* **114:** 37–50

Wright WE, Binder M, Funk W (1991) Cyclic amplification and selection of targets (CASTing) for the myogenin consensus binding site. *Mol Cell Biol* **11:** 4104–4110

Yin T, Green KJ (2004) Regulation of desmosome assembly and adhesion. *Semin Cell Dev Biol* **15:** 665–677

Zhao Q, Cumming H, Cerruti L, Cunningham JM, Jane SM (2004) Site-specific acetylation of the fetal globin activator NF-E4 prevents its ubiquitination and regulates its interaction with the histone deacetylase, HDAC1. *J Biol Chem* **279:** 41477–41486

Zhong W, Sternberg PW (2006) Genome-wide prediction of C. elegans genetic interactions. *Science* **311:** 1481–1484

©2008 European Molecular Biology Organization